



Parametric excitation of eigenmodes in microscopic magnetic dots

Henning Ulrichs,^{*} Vladislav E. Demidov, and Sergej O. Demokritov

Institute for Applied Physics and Center for Nonlinear Science, University of Muenster, Corrensstrasse 2-4, 48149 Muenster, Germany

Sergei Urazhdin

Department of Physics, West Virginia University, Morgantown, WV 26506, USA

(Received 22 June 2011; published 2 September 2011)

We utilize time- and space-resolved Brillouin light scattering spectroscopy to study the parametric excitation of spin-wave eigenmodes in microscopic Permalloy dots. We show that the fundamental center eigenmode has the smallest excitation threshold. With the increase of the pumping power above this threshold, higher-order dipole-dominated eigenmodes with both even and odd spatial symmetry also become excited. At microwave power levels far above the threshold, the multimode excitation regime is suppressed due to the parametric excitation of short-wavelength exchange-dominated spin-wave modes. Our results provide important insight into the physics of parametric processes in microscopic magnetic systems.

DOI: [10.1103/PhysRevB.84.094401](https://doi.org/10.1103/PhysRevB.84.094401)

PACS number(s): 75.40.Gb, 85.75.-d, 75.30.Ds, 75.75.-c

I. INTRODUCTION

Parametric processes in magnetic systems were observed by Bloembergen and Damon¹ and theoretically explained by Anderson and Suhl² more than 50 years ago. Since then, they have been intensively studied in the context of applied physics as well as basic research.^{3–15} Parametric processes can be utilized for amplification and manipulation of spin-wave pulses,^{7–9} parametric stimulation and recovery of microwave signals,¹⁰ and wave-front reversal.¹¹ They also can be used as a powerful experimental tool in studies of spin-wave solitons and two-dimensional bullets,^{7,8,12,13} as well as magnon Bose-Einstein condensates.^{14,15}

One of the main parameters governing the efficiency of parametric excitation is dynamic damping.¹⁶ Monocrystalline yttrium iron garnet (YIG) films are characterized by extremely low magnetic damping (Gilbert damping parameter $\alpha < 10^{-4}$) and thus have become the material of choice for studies of parametric excitation and amplification of magnetization oscillations and waves. As a consequence of the low damping in YIG, moderate microwave pumping levels are sufficient for parametric excitation, enabling studies of strongly nonequilibrium states such as parametrically driven magnon gas in strongly nonlinear regimes.¹⁷

As a material for technical applications, YIG has several drawbacks. High-quality YIG films can be grown only on special substrates, such as gallium gadolinium garnet, which makes the fabrication process incompatible with conventional silicon-based semiconductor technology. Additionally, this material is difficult to structure, and it also exhibits a strong dependence of the magnetic properties on temperature due to the relatively low Curie point. In contrast, polycrystalline transition-metal ferromagnetic films can be easily grown by sputtering or evaporation on a variety of substrates, including silicon, and they can be structured on a submicrometer scale by standard lithography techniques. Among these materials, $\text{Ni}_{80}\text{Fe}_{20}$ = Permalloy (Py) is most widely used for basic research and applied studies due to its low crystalline anisotropy and small damping ($\alpha < 10^{-2}$). Py has been utilized as a working medium in spin-

torque nano-oscillators,^{18–21} magnonic crystals,^{22–26} domain wall motion-based memory devices,²⁷ and spin-wave logic circuits.²⁸

Magnetic damping in Py is relatively small compared to other metallic ferromagnets, but it is still much larger than in YIG, resulting in a significantly higher threshold power required for parametric excitation. For instance, parametric excitation of spin waves in Permalloy films has been achieved only with microwave power levels of at least a few Watts.^{29,30} This problem can be overcome by reducing the dimensions of the magnetic samples to nanometer scale and concentrating the pumping energy into a smaller volume, thus producing a large local microwave field sufficient for parametric excitation using moderate driving power.^{31,32}

In this paper, we report an experimental investigation of the parametric excitation of spin-wave modes in an elliptical Py dot with submicrometer dimensions fabricated on top of a microscopic microwave transmission line. To analyze the spectral and spatial characteristics of the excited modes, we utilized time- and space-resolved microfocus Brillouin light scattering (BLS) spectroscopy.³³ The parametric excitation threshold power of about 1 mW was significantly smaller than in the extended Py films, enabling us to investigate parametric excitation processes far above the threshold. We show that above the threshold, many different dipole-dominated eigenmodes can be excited. At large parametric pumping power, short-wavelength exchange-dominated spin-wave modes also become excited. The transfer of the parametric pumping energy into the short-wavelength part of the mode spectrum results in a decreased excitation efficiency of the dipole-dominated modes. This redistribution of energy does not significantly affect the excitation of the lowest-frequency modes of the dot. Consequently, the fundamental center and the edge modes can be efficiently excited by the parametric pumping both at small and at large pumping power levels. These results are important for the development of integrated magnetic devices utilizing parametric processes for excitation and amplification of magnetization oscillations.

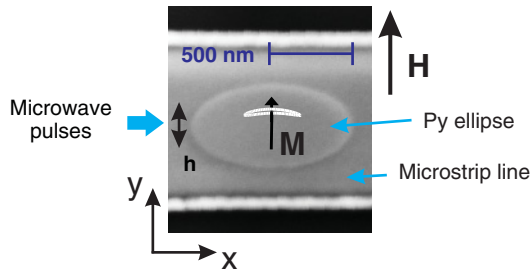


FIG. 1. (Color online) Scanning electron micrograph of the sample.

II. SAMPLE AND MEASUREMENT SETUP

Figure 1 shows a scanning electron micrograph of the studied sample, which consists of a 10-nm-thick Py film patterned by electron-beam lithography and ion milling into an elliptical dot with lateral dimensions of 1000 by 500 nm. The dot is fabricated directly on top of a 1- μm -wide and 160-nm-thick Au microstrip transmission line. A static magnetic field of $H = 400\text{--}700$ Oe was applied along the short axis of the Py ellipse. The data presented here were obtained at $H = 700$ Oe. To excite the magnetization dynamics, microwave pulses with duration of 100 ns and a repetition period of 2 μs were applied to the transmission line. The pulse power was varied between 0.1 mW and 50 mW. The microwave pulses created a dynamic magnetic field \mathbf{h} parallel to the direction of the static magnetization.

The detection of the magnetization dynamics was performed by microfocus BLS technique described in detail in Ref. 33. This technique combines the spectral and temporal resolution of the conventional BLS³⁴ with diffraction-limited spatial resolution of about 250 nm determined by the size of the probing laser spot. The intensity of the scattered light at a given frequency is proportional to the square of the dynamic magnetization amplitude at this frequency, at the position of the probing spot.

The dynamic magnetic field \mathbf{h} was parallel to the static magnetization in our experimental geometry. In this configuration, the microwave field cannot linearly excite magnetization dynamics, since the corresponding component of the dynamic magnetic susceptibility tensor is equal to zero.¹⁶ Instead, the dynamics can be excited by a higher-order parametric excitation process.³⁵ In the quasiparticle picture, this process can be understood as splitting of a microwave photon with frequency f_p and wave vector $k_p \approx 0$ into two magnons with frequency $f_p/2$ and wave vectors that are equal in magnitude and opposite in direction.¹⁶ In accordance with this picture, in our experiments, we detected magnetization oscillations at half of the applied microwave pumping frequency f_p .

In confined sample geometries, quantization of the spin-wave spectrum imposes limitations on the parametric excitation. Specifically, the dynamic magnetization response exhibits resonant spectral behavior, with resonant frequencies equal to those of the system's eigenmodes. By utilizing the spectral sensitivity of the BLS technique to detect only the dynamic signal at the frequency of a particular mode, one can selectively map out its spatial profile. Additionally, by synchronizing the microwave pulses with the spectrometer clock, the time

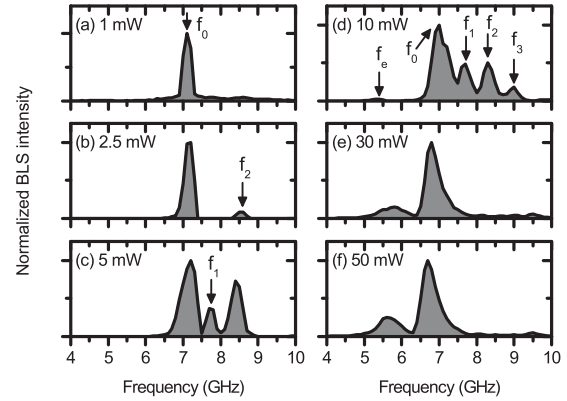


FIG. 2. BLS spectra recorded at powers of parametric pumping varying from 1 to 50 mW, as labeled. The horizontal scale is the detection frequency, equal to half of the pumping frequency.

dependence of the magnetization response to the excitation pulses can be recorded with resolution of 1 ns.

III. EXPERIMENTAL RESULTS AND ANALYSIS

A. Spectral characteristics of parametric excitation

Figure 2 shows the BLS spectra recorded at different values of the microwave pumping power P between 1 and 50 mW, providing a survey of the spectroscopic properties and power-dependent dynamical regimes of the system. To record the spectra, the laser spot was positioned at the center of the Py dot. The pumping frequency f_p was varied between 8 and 20 GHz, and the BLS intensity was simultaneously measured at $f_p/2$.

Because of the threshold nature of the parametric excitation, no dynamic magnetization was detected at $P < 1$ mW. At $P = 1$ mW, the spectrum exhibits a single peak at $f_0 = 7.1$ GHz ($f_p = 14.2$ GHz), corresponding to the spin-wave eigenmode with the lowest parametric threshold [Fig. 2(a)]. At $P > 2$ mW, a second peak appears at $f_2 = 8.5$ GHz, as illustrated in Fig. 2(b) for $P = 2.5$ mW. At $P > 3.2$ mW, a third peak appears at $f_1 = 7.7$ GHz, as illustrated in Fig. 2(c) for $P = 5$ mW. At even larger power levels, several additional peaks appeared in the spectra. For example, four closely spaced large peaks and an additional small peak at frequency f_e significantly below f_0 can be distinguished at $P = 10$ mW [Fig. 2(d)]. There is also a bump on the declining slope of the peak at f_0 , suggesting that at least one additional mode with frequency close to f_0 may be excited.

This simple trend is reversed at excitation powers above 10 mW. The BLS spectra now exhibit only two peaks at frequencies f_0 and f_e [Figs. 2(e) and 2(f)]. These two peaks exhibit a nonlinear frequency shift with increasing P . In addition, they broaden and become noticeably asymmetric. The asymmetry is especially pronounced for the peak at f_0 , which clearly has a significantly steeper rising slope than the declining slope, characteristic for a nonlinear resonance.^{36–38}

B. Spatial characteristics of the parametrically excited modes

To identify the normal modes associated with the observed spectral peaks, we performed spatially resolved measurements

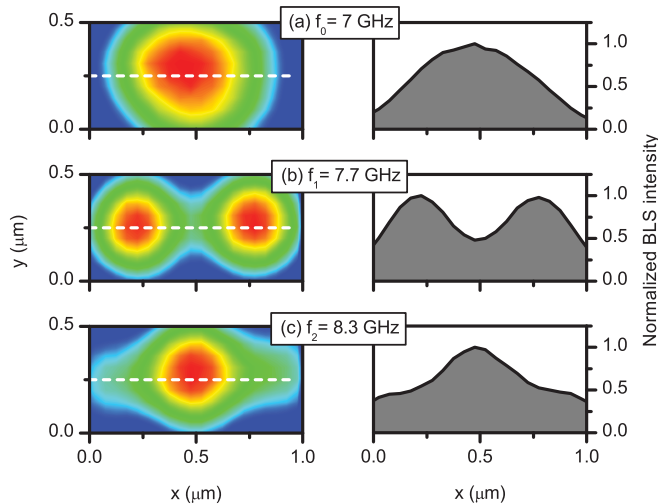


FIG. 3. (Color online) Left: Pseudocolor-coded maps of the BLS intensity. Right: One-dimensional cross sections of the maps along the major axis of the Py ellipse, as marked by the dashed lines. Panels (a)–(c) were acquired at the labeled frequency values corresponding to three different spectral peaks.

at $P = 10$ mW, where the largest numbers of peaks are observed. For each of the observed peaks, the excitation frequency was fixed at twice its central frequency, and two-dimensional mapping of the BLS intensity was performed. The probing spot was scanned in x - and y -directions with a step size of 50 nm across a 500 by 1000 nm rectangular area covering the Py dot. The left-side panels in Fig. 3 show pseudocolor-coded maps of the recorded BLS intensity. The right-side panels show one-dimensional cross sections of these maps along the major axis of the Py ellipse. It is important to note that the measured two-dimensional maps and one-dimensional profiles represent a result of convolution of the local dynamic magnetization amplitude with the instrumental resolution function, resulting in a significant blurring of submicrometer spatial features.

Figure 3(a) shows that the mode at frequency $f_0 = 7$ GHz has a half-sine profile along the major axis, and it does not exhibit any nodal lines. These characteristics indicate that it is the fundamental center mode of the Py dot.³⁹ The profile of the mode at frequency $f_1 = 7.7$ GHz [Fig. 3(b)] has two maxima on the long axis and a minimum at the center of the dot. This minimum is likely associated with the nodal line of the eigenmode. The BLS intensity does not vanish at the minimum, likely due to the limited spatial resolution of our technique.

The spatial profile of the mode at $f_2 = 8.3$ GHz [see Fig. 3(c)] has a maximum at the center, similar to the fundamental mode. In contrast to that mode, the profile is sharper near the maximum, and it forms two broad shoulders with small bumps near the edges. As mentioned previously, fine spatial features are blurred due to finite resolution of the setup. Therefore, based on our data, the mode with the frequency f_2 can be interpreted as a mode with two nodal lines separating a central maximum from two side maxima located on the major axis of the Py ellipse.

The limitations of the spatial resolution of our technique prevented us from identifying the mode corresponding to the peak at f_3 . This higher-order mode likely has three nodal

lines. We also performed spatially resolved measurements at $f_e = 5.5$ GHz, which revealed a typical spatial structure of the so-called edge mode, with maxima of intensity close to the edges of the dot on the axis parallel to the direction of the static field, and a vanishing intensity at the center of the dot.

We note that the mode observed at $f_1 = 7.7$ GHz [Fig. 3(b)] is expected to have odd spatial symmetry, i.e., its amplitude profile is antisymmetric with respect to the minor axis of the dot. By symmetry, this mode cannot be directly excited by the usual linear excitation mechanism with a spatially uniform dynamic magnetic field. The symmetry of the mode at f_2 does not prohibit its linear excitation by a uniform field, but the excitation efficiency would be significantly smaller than for the fundamental mode at f_0 .⁴⁰ In contrast, the efficiency of parametric excitation for all these modes is similar, as indicated by the similar amplitudes of the peaks in Fig. 2(d). Therefore, the parametric excitation mechanism presents significant advantages compared to linear excitation for the experimental studies of the eigenmode spectra in micro- and nanomagnets.

C. Dependence of the mode intensities on pumping power

We now analyze and interpret the dependencies of the parametrically excited mode intensities on the pumping power. Figure 4 shows these dependencies for the fundamental mode (filled triangles), the higher-order mode at f_2 (open triangles), and the edge mode at f_e (circles). Both of the center modes exhibit similar nonmonotonic behavior above their excitation thresholds: The intensities first increase and then start to decrease with further increases in the pumping power. The intensity of the fundamental mode reaches a minimum at $P \approx 6$ mW and then increases again. In contrast, the BLS peak at f_2 becomes indistinguishable from the background at $P = 12$ mW and does not recover at larger pumping powers. Similar behaviors were also observed for the higher-order modes at frequencies f_1 and f_3 .

These data suggest the presence of a mechanism limiting the energy flow from the parametric pumping to the observed

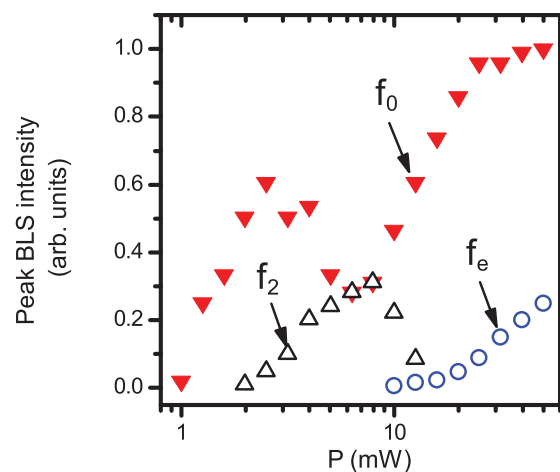


FIG. 4. (Color online) Dependence of the BLS peak intensity on pumping power for the fundamental mode at f_0 (filled triangles), for the higher-order mode at f_2 (open triangles), and for the edge mode at f_e (open circles).

modes at large P . Although this mechanism influences all the observed modes, its effect on the higher-order modes is stronger than on the fundamental mode, leading to their complete suppression.

To interpret these behaviors, we recall that because of the intrinsic anisotropy of the magnetic eigenmode spectrum, the frequencies of the modes only weakly depend on the number of nodal lines perpendicular to the magnetization.⁴¹ As a consequence, for each mode with nodal lines parallel to the static magnetization (see Fig. 3), there are, generally speaking, many nearly degenerate modes with a finite number of nodal lines perpendicular to the magnetization. For example, at frequencies f_1 – f_3 , there are a number of exchange-dominated modes with very short effective wavelengths in the direction parallel to magnetization. These modes cannot be detected by the BLS technique, which is sensitive predominantly to the long-wavelength modes.

The exchange-dominated modes are generally characterized by stronger damping and weaker coupling to the pumping field, and consequently they have larger excitation thresholds compared to the dipole-dominated modes.⁴¹ Therefore, only the dipole-dominated modes are excited at small P , and, in this regime, their intensity increases with P . As P reaches the threshold value for the excitation of the exchange-dominated modes, additional scattering channels become effective that redistribute the energy among the modes. While the details of these processes are presently unknown, one can generally expect that the increase in the amplitudes of exchange-dominated magnetization oscillations results in nonlinear scattering of the dipole-dominated oscillations into the short-wavelength part of the mode spectrum, creating additional nonlinear damping channels for the dipole-dominated modes. As a result, the flow of energy from the pumping to the dipole-dominated modes decreases, leading to a decrease of their intensity and, at sufficiently large pumping power, to the complete suppression of the dipole-dominated modes.

This suppression mechanism is significantly less efficient for the fundamental mode, since it has the lowest frequency among the center modes, and consequently there are no exchange-dominated modes at the same frequency. Nevertheless, there are a number of modes with no nodal lines parallel to the magnetization and several nodal lines perpendicular to the magnetization whose frequency is only slightly different from that of the fundamental mode. The onset of their parametric excitation can be the origin of the decrease in the fundamental peak intensity at $P > 3$ mW.

These modes are dipole dominated and thus should be detectable by the BLS measurements. Indeed, the broadening of the fundamental peak at $P > 3$ mW [compare Fig. 2(a) and 2(c)] and a bump on its declining slope [see Fig. 2(d)] can be interpreted as a signature of their excitation. In addition, in the interval $P = 3$ – 8 mW, spatially resolved measurements revealed deviations of the spatial profile of the mode at f_0 from that shown in Fig. 3(a) for $P = 10$ mW, which can be associated with simultaneous excitation of several dipole-dominated modes with different spatial profiles. The largest deviations were observed at $P = 6$ mW, corresponding to the minimum of the fundamental mode intensity. These deviations are dramatically reduced at $P > 10$ mW. Based on these data, one can conclude that, in contrast to the competition between

the dipole-dominated and exchange-dominated modes, the competition among the dipole-dominated modes results in the predominant energy flow into the fundamental mode of the dot at large P .

Finally, the intensity of the edge mode (circles in Fig. 4) increases monotonically with increasing P . This behavior is consistent with the intensity-suppression mechanisms discussed already: since the frequency of the edge mode lies far below the frequencies of all the other modes of the system, its intensity is not affected by their parametric excitation.

D. Temporal characteristics of parametric excitation

In addition to the significance of parametric excitation as a spectroscopic tool, it can be used to determine other important dynamical parameters of the magnetic system. The time dependence of the excited mode amplitude at different pumping powers provides information about the magnetic damping constant, the strength of the microwave pumping field, and its coupling to the magnetic system (see Sec. IV for details).

We performed time-resolved measurements of the fundamental mode intensity at pumping powers between the threshold value of 1 mW and 50 mW, with temporal resolution of 1 ns. Figures 5(a) and 5(b) show time traces for $P = 1$ mW and 3.2 mW. These data demonstrate that just above the parametric threshold, the rate of intensity growth is small, but it quickly increases with increasing P .

Plotting the time-dependent intensity of the fundamental mode on the logarithmic scale, at $P = 1$ – 4 mW, we observe a well-defined initial exponential rise followed by saturation, as illustrated in Fig. 5(c) for $P = 3.2$ mW. Fitting this exponential dependence, we obtain a characteristic rise time constant τ as a function of the pumping power for $P < 4$ mW. At larger powers, $P > 4$ mW, the intensity growth becomes too abrupt to make a reliable estimate of τ due to the limited temporal resolution

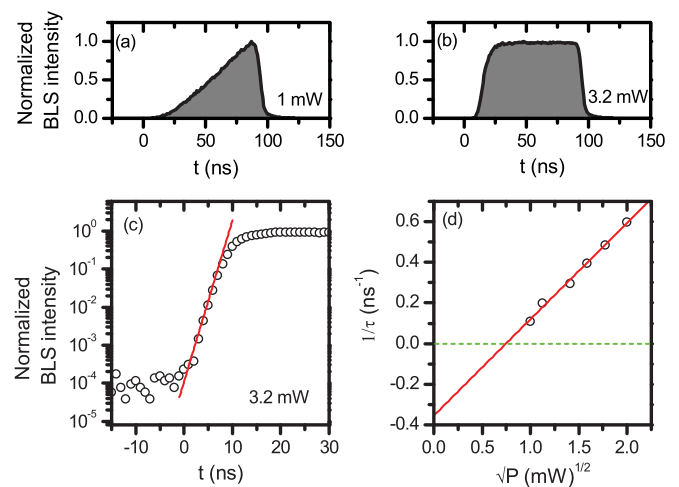


FIG. 5. (Color online) (a) and (b) Time traces of the fundamental mode intensity at the labeled values of pumping power; $t = 0$ corresponds to the start of the pumping pulse. (c) Time dependence of intensity on the logarithmic scale at $P = 3.2$ mW. Line shows the result of a fit by an exponential function. (d) The inverse of amplitude rise time constant vs $\sqrt{P} \propto h$. Line is the best linear fit of the data.

of our measurement. Analysis given in Sec. IV suggests that the inverse of the time constant τ should depend linearly on h , which is proportional to the square root of the pumping power, $h = A\sqrt{P}$. Here, A is a calibration parameter determined by the sample geometry and the microwave losses in the transmission line. As expected, the experimentally determined values of $1/\tau$ follow a linear dependence on \sqrt{P} [Fig. 5(d)].

IV. THEORY

Rigorous understanding of the nonlinear dynamical regimes in microscopic structures requires a self-consistent theory of parametric excitation taking into account the effects of the inhomogeneity of the internal demagnetizing field and the magnetization in the sample, as well as the boundary conditions governing spin-wave quantization. Nevertheless, the theory developed for extended magnetic films⁴¹ can still be used to analyze the behavior of the studied system close to the threshold of parametric excitation. According to Ref. 41, the threshold amplitude of the dynamic magnetic field for the onset of parametric excitation is given by

$$h_{\text{th}} = \omega_r/V, \quad (1)$$

where $\omega_r = \alpha\omega$ is the relaxation frequency, and $V = \gamma^2 4\pi M_s [P(k)(1 + \sin^2(\varphi)) - 1]/(4\omega)$ is a coefficient characterizing the coupling of the pumping field to the plane wave with frequency ω and wave vector \mathbf{k} oriented in the film plane at an angle φ with respect to the direction of the static magnetization: $\varphi = \tan^{-1}(k_y/k_x)$. Here, $4\pi M_s$ is the saturation magnetization, and $P(k) = 1 - (1 - \exp[-kd])/kd$, where d is the film thickness.

To account for the finite lateral dimensions of the dot, we applied the standard spin-wave quantization scheme.⁴² Within this approach, the fundamental center mode of the dot is approximated by a two-dimensional standing spin wave with the components of the wave vector $k_x = \pi/a$ and $k_y = \pi/b$, where $a = 1000$ nm and $b = 500$ nm, which represent the lateral sizes of the dot in the x and y directions, respectively. In this approximation, the coupling coefficient is $V = 1.63 \times 10^7$ (Oe·s)⁻¹.

Above the threshold, the amplitude of the parametrically excited mode is expected to grow exponentially with a characteristic time constant (see Ch. 5.3 in Ref. 43)

$$\tau = 1/(hV - \omega_r). \quad (2)$$

In agreement with this result, the experimental values for $1/\tau$ scale linearly with h [Fig. 5(d)]. As follows from Eq. (2), $1/\tau$ is equal to the relaxation frequency ω_r at $h = 0$ and vanishes at $h = h_{\text{th}}$. Fitting the experimental data of Fig. 5(d) with a linear function and extrapolating to $P = 0$, we obtain $\omega_r = 0.36 \times 10^9$ s⁻¹, corresponding to the Gilbert damping parameter $\alpha = 0.008$, which is in excellent agreement with the known value for Py.⁴⁴ From the same fit, we also obtain the threshold power $P_{\text{th}} = 0.6$ mW, corresponding to exact compensation of the magnetic relaxation by the parametric pumping. Finally, from the slope of the linear dependence, we obtain the calibration factor $A = 29$ Oe/(mW)^{1/2}. This value is in reasonable agreement with the estimate $A = 24$ Oe/(mW)^{1/2} based on the nominal geometrical parameters of the microstrip line.

V. CONCLUSIONS

In conclusion, we have demonstrated parametric excitation of spin-wave modes in microscopic magnetic-film structures at moderate microwave powers. Parametric processes can be utilized for studies of the eigenmode spectra and other dynamical characteristics in micro- and nanomagnets. The low threshold power for parametric excitation in microscopic systems enables observation of complex nonlinear phenomena such as mode competition and nonlinear parametric resonance. Moreover, the low threshold power makes parametric processes in microscopic structures useful for technical applications such as parametric amplification of spin waves in integrated magnonic devices.

ACKNOWLEDGMENTS

We acknowledge support from Deutsche Forschungsgemeinschaft, the European Project Master (No. NMP-FP7 212257), National Science Foundation (NSF) Grant Nos. DMR-0747609 and ECCS-0967195, and the Research Corporation.

*henning.ulrichs@uni-muenster.de

¹N. Bloembergen, and R. W. Damon, *Phys. Rev.* **85**, 699 (1952).

²P. W. Anderson, and H. Suhl, *Phys. Rev.* **100**, 1788 (1955).

³V. E. Zakharov, V. S. Lvov, and S. S. Starobinets, *Sov. Phys. JETP* **32**, 656 (1971).

⁴V. N. Venitskii, V. V. Eremenko, and E. V. Matyushkin, *Sov. Phys. JETP* **50**, 934 (1979).

⁵W. Wettleing, W. D. Wilber, P. Kabos, and C. E. Patton, *Phys. Rev. Lett.* **51**, 1680 (1983).

⁶P. Kabos, C. E. Patton, G. Wiese, A. D. Sullins, E. S. Wright, and L. Chen, *J. Appl. Phys.* **80**, 3962 (1996).

⁷A. V. Bagada, G. A. Melkov, A. A. Serga, and A. N. Slavin, *Phys. Rev. Lett.* **79**, 2137 (1997).

⁸P. A. Kolodin, P. Kabos, C. E. Patton, B. A. Kalinikos, N. G. Kovshikov, and M. P. Kostylev, *Phys. Rev. Lett.* **80**, 1976 (1998).

⁹K. R. Smith, V. I. Vasyuchka, M. Wu, G. A. Melkov, and C. E. Patton, *Phys. Rev. B* **76**, 054412 (2007).

¹⁰A. A. Serga, A. V. Chumak, A. André, G. A. Melkov, A. N. Slavin, S. O. Demokritov, and B. Hillebrands, *Phys. Rev. Lett.* **99**, 227202 (2007).

¹¹A. L. Gordon, G. A. Melkov, A. A. Serga, A. N. Slavin, V. S. Tiberkevich, and A. V. Bagada, *JETP Lett.* **67**, 913 (1998).

¹²S. O. Demokritov, A. A. Serga, V. E. Demidov, B. Hillebrands, M. P. Kostylev, and B. A. Kalinikos, *Nature* **426**, 159 (2003).

- ¹³A. A. Serga, B. Hillebrands, S. O. Demokritov, A. N. Slavin, P. Wierzbicki, V. Vasyuchka, O. Dzyapko, and A. Chumak, *Phys. Rev. Lett.* **94**, 167202 (2005).
- ¹⁴S. O. Demokritov, V. E. Demidov, O. Dzyapko, G. A. Melkov, A. A. Serga, B. Hillebrands, and A. N. Slavin, *Nature* **443**, 430 (2006).
- ¹⁵V. E. Demidov, O. Dzyapko, M. Buchmeier, T. Stockhoff, G. Schmitz, G. A. Melkov, and S. O. Demokritov, *Phys. Rev. Lett.* **101**, 257201 (2008).
- ¹⁶A. G. Gurevich, and G. A. Melkov, *Magnetization Oscillation and Waves* (CRC Press, Boca Raton, FL, 1996).
- ¹⁷V. E. Demidov, O. Dzyapko, S. O. Demokritov, G. A. Melkov, and A. N. Slavin, *Phys. Rev. Lett.* **99**, 037205 (2007).
- ¹⁸I. N. Krivorotov, N. C. Emley, J. C. Sankey, S. I. Kiselev, D. C. Ralph, and R. A. Buhrman, *Science* **307**, 228 (2005).
- ¹⁹F. B. Mancoff, N. D. Rizzo, B. N. Engel, and S. Tehrani, *Nature* **437**, 393 (2005).
- ²⁰M. R. Puffall, W. H. Rippard, S. E. Russek, S. Kaka, and J. A. Katine, *Phys. Rev. Lett.* **97**, 087206 (2006).
- ²¹V. E. Demidov, S. Urazhdin, and S. O. Demokritov, *Nat. Mater.* **9**, 984 (2010).
- ²²S. Neusser, and D. Grundler, *Adv. Mat.* **21**, 2927 (2009).
- ²³V. V. Kruglyak, P. S. Keatley, A. Neudert, R. J. Hicken, J. R. Childress, and J. A. Katine, *Phys. Rev. Lett.* **104**, 027201 (2010).
- ²⁴S. Tacchi, M. Madami, G. Gubbiotti, G. Carlotti, H. Tanigawa, T. Ono, and M. P. Kostylev, *Phys. Rev. B* **82**, 024401 (2010).
- ²⁵A. V. Chumak, P. Pirro, A. A. Serga, M. P. Kostylev, R. L. Stamps, H. Schultheiss, K. Vogt, S. J. Hermsdoerfer, B. Laegel, P. A. Beck, and B. Hillebrands, *Appl. Phys. Lett.* **95**, 262508 (2009).
- ²⁶Z. K. Wang, V. L. Zhang, H. S. Lim, S. C. Ng, M. H. Kuok, S. Jain, and A. O. Adeyeye, *Appl. Phys. Lett.* **94**, 083112 (2009).
- ²⁷S. S. P. Parkin, M. Hayashi, and L. Thomas, *Science* **320**, 5873 (2008).
- ²⁸A. Khitun, M. Bao, and K. L. Wang, *J. Phys. D: Appl. Phys.* **43**, 264005 (2010).
- ²⁹S. Y. An, P. Krivosik, M. A. Kramer, H. M. Olson, A. V. Nazarov, and C. E. Patton, *J. Appl. Phys.* **96**, 1572 (2004).
- ³⁰G. A. Melkov, Yu. V. Koblyanskiy, R. A. Slipets, A. V. Talalaevskij, and A. N. Slavin, *Phys. Rev. B* **79**, 134411 (2009).
- ³¹V. E. Demidov, H. Ulrichs, S. O. Demokritov, and S. Urazhdin, *Phys. Rev. B* **83**, 020404(R) (2011).
- ³²S. Urazhdin, V. S. Tiberkevich, and A. N. Slavin, *Phys. Rev. Lett.* **105**, 237204 (2010).
- ³³S. O. Demokritov, and V. E. Demidov, *IEEE Trans. Magn.* **44**, 6 (2008).
- ³⁴S. O. Demokritov, B. Hillebrands, and A. N. Slavin, *Phys. Rep.* **348**, 441 (2001).
- ³⁵E. Schlömann, J. J. Green, and U. Milano, *J. Appl. Phys.* **31**, S386 (1960).
- ³⁶T. Gerrits, P. Krivosik, M. L. Schneider, C. E. Patton, and T. J. Silva, *Phys. Rev. Lett.* **98**, 207602 (2007).
- ³⁷Y. S. Gui, A. Wirthmann, and C.-M. Hu, *Phys. Rev. B* **80**, 184422 (2009).
- ³⁸Y. Khivintsev, B. Kuanr, T. J. Fal, M. Haftel, R. E. Camley, Z. Celinski, and D. L. Mills, *Phys. Rev. B* **81**, 054436 (2010).
- ³⁹I. Neudecker, K. Perzmaier, F. Hoffmann, G. Woltersdorf, M. Buess, D. Weiss, and C. H. Back, *Phys. Rev. B* **73**, 134426 (2006).
- ⁴⁰V. E. Demidov, M. P. Kostylev, K. Rott, P. Krzysteczko, G. Reiss, and S. O. Demokritov, *Appl. Phys. Lett.* **95**, 112509 (2009).
- ⁴¹D. N. Chartoryzhskii, B. A. Kalinikos, and O. G. Vendik, *Solid State Commun.* **20**, 985 (1976).
- ⁴²K. Yu. Guslienko, S. O. Demokritov, B. Hillebrands, and A. N. Slavin, *Phys. Rev. B* **66**, 132402 (2002).
- ⁴³V. S. L'vov, *Wave Turbulence under Parametric Excitation* (Springer-Verlag, Berlin-Heidelberg, 1994).
- ⁴⁴J. O. Rantschler, R. D. McMichael, A. Castillo, A. J. Shapiro, W. F. Egelhoff Jr., B. B. Maranville, D. Pulugurtha, A. P. Chen, and L. M. Connors, *J. Appl. Phys.* **101**, 033911 (2007).